Studies of Drag-Reduction Methods for Subsonic Operation of Supersonic Inlets

GEORGE L. MULLER* AND WILLIAM F. GASKO†
Pratt & Whitney Aircraft, East Hartford, Conn.

Two schemes were studied in an attempt to reduce the drag of a supersonic inlet at subsonic speeds. One of the methods is to use a retractable airfoil in front of the cowl to generate thrust. The second method involves hinging the cowl lip inward so that the captured airflow is choked, thus lowering the pressures on the external surfaces. Both schemes were successful in reducing the drag at captured airflow rates less than the choking point of the plain inlet. Although the drag was not reduced below the critical drag of the plain inlet, the tests indicate that this may be possible.

Nomenclature

A_e = nozzle-exit flow area
A_i = inlet flow area at cowl lip
$A_{\max}$ = maximum inlet frontal area
A_0 = freestream tube area of captured flow
A_1 = inlet capture area
A_2 = inlet throat area (equal to A_i for subsonic-transonic operation)
C_c = cowl pressure drag coefficient
$C_{D\text{add}}$ = additive drag coefficient
D_{add} = additive drag
D_B = boattail or afterbody drag
D_{cb} = centerbody pressure drag
D_{ext} = external pressure drag
D_{tot} = sum of additive and forebody drag (including airfoils)
D_f = friction drag
D_w = wave or forebody drag (not including D_{cb})
e = exit station
ext = external part
ext_{cb} = external part of centerbody
F_A = maximum available net thrust
F_p = propulsion force exerted on aircraft
F_{bal} = force on drag balance
i = inlet cowl station
int = internal part
m_a = engine mass flow
m_e = mass flow leaving exit
m_i = mass flow entering cowl lip station
m_0 = mass flow in freestream tube enclosing captured flow
M_0 = freestream Mach number
$\bar{P}_e$ = area-weighted average pressure at nozzle exit; $= \int_e p dA/A_e$
P_{ext} = external pressure
P_i = average pressure at cowl lip
P_{int} = internal pressure
P_0 = freestream pressure
$(PA)_{\text{base}}$ = force on base of drag balance
$(PA)_{\text{step}}$ = force on step between balance and model outer diameters
$\bar{v}_e$ = mass flow-weighted average velocity at exit; $= \int_e v dm/m_e$
v_0 = freestream velocity
γ = ratio of specific heats

Introduction

IT is becoming increasingly important that the engine manufacturer be able to predict installation effects on engine performance. This occurs because today's high-performance aircraft can impose greater installation losses. Inlet drag at off-design speeds is one type of installation loss. As the off-design requirements for supersonic aircraft increase, reduction of off-design inlet drag becomes a worthwhile goal. Perhaps compromises in inlet design are required to meet this goal.

When a supersonic inlet is operated at subsonic speed, its drag is significantly higher than the drag of a subsonic inlet designed for that speed. Part of this increase in drag is due to the increased capture area of the supersonic inlet caused by the centerbody, and by the fact that the capture area is sized for supersonic cruise. The balance of the increase is due to the fact that subsonic inlets rely on low pressure (lip suction) around a blunt cowl to reduce the drag, whereas supersonic inlets have sharp cowls, which cause flow separation that considerably reduces the suction.

Similarly, the drag of inlets designed for subsonic flight will be much greater at supersonic speeds than the drag of a supersonic inlet because of wave drag on the blunt cowl. Obviously, some compromises between subsonic and supersonic inlet design are required for the inlet to operate reasonably well in both subsonic and supersonic flight.

This study examined two compromises that might be made. Both involved the modification of an axisymmetric supersonic inlet for subsonic flight. The two compromises were 1) to add a retractable blunt-lip airfoil in front of the cowl for subsonic operation, and 2) to reduce the capture area by hinging the cowl lip inward at subsonic speeds.

During the course of this study, a report was obtained describing work on reduction of transonic additive drag of some two-dimensional supersonic inlets.[4] Here, as well, a hinged cowl was used to reduce drag. Various cowl shapes were investigated.

Since the emphasis in this test program was placed on drag measurements, no effort was made to obtain good pressure recovery or low distortion. These are governed by other criteria beyond the scope of this program and do not significantly affect the drag.

Theoretical Considerations

Additive Drag Concept

The concept of additive drag arises as a consequence of the force bookkeeping system used by industry to evaluate the force exerted on the aircraft by the propulsion system. Here, the engine manufacturer supplies specifications on the maximum available net thrust F_A, which is defined as the propulsion system thrust. For this discussion, there is no need to consider bleed or bypass flow, so that the captured flow equals the engine flow. Thus, the force exerted on the air-

Received October 7, 1966; revision received April 13, 1967. The major portion of this work was conducted for the United States Air Force Systems Command, Wright-Patterson Air Force Base under Contract AF33(657)14903. [3.01, 3.01, 4.02]

* Assistant Project Engineer, Inlet Research and Technology. Member AIAA.

† Senior Engineer, Inlet Research and Technology. Member AIAA.

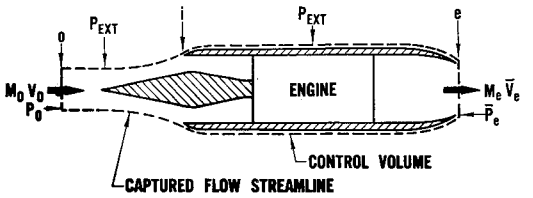

Fig. 1 Pressure and momentum terms in engine installation.

craft is then given by

$$F_p = F_A - D_{\text{add}} - D_{\text{ext}} \tag{1}$$

$$F_A = m_e \bar{v}_e + (\bar{P}_e - P_0)A_e - m_0 v_0 \tag{2}$$

where, neglecting friction,

$$D_{\text{add}} = \int_0^i (P_{\text{ext}} - P_0)dA \tag{3}$$

$$D_{\text{ext}} = \int_i^e (P_{\text{ext}} - P_0)dA \tag{4}$$

Figure 1 illustrates the pressure and momentum terms used in the foregoing equations.

The aircraft manufacturer usually supplies the drag integrals, as these are a function of the aircraft design. If we separate the external drag into forebody and afterbody drag,

$$F_p = F_A - D_{\text{add}} - D_w - D_B \tag{5}$$

For the limiting case of perfect flow (potential, isentropic flow), the sum of the additive and forebody drag is zero.

Thus, it is the irreversibilities in the flow—viscosity, shock waves, and separation—which cause "spillage" drag (the sum of the additive and forebody drag). If cowls for subsonic inlets are designed with blunt leading edges and smoothly curved forebodies, separated flow can be avoided or held to a minimum. The suction generated by the forebody nearly cancels the additive drag. Supersonic cowls, however, must be sharp to have low wave drag at supersonic speeds. At subsonic speeds, the sharp edge separates the flow so that little forebody suction is generated. Figure 2 summarizes the differences between subsonic and supersonic inlets.

Theory of Airfoil Operation

One of the possibilities for reducing drag of supersonic inlets at subsonic speeds is the retractable airfoil. The airfoil is extended in front of the cowl at subsonic speeds and, at supersonic speeds, is collapsed and retracted into the cowl, as shown in Fig. 3. Figure 4 defines the flow regimes where thrust can be attained from the airfoil. As the local flow angle decreases, higher lift-drag ratios are required to obtain thrust. This decrease in flow angle corresponds to an increase in captured mass flow so that the amount of thrust generated by the airfoil decreases as the mass flow increases. Fortunately,

a) Subsonic inlet: lip suction reduces effect of additive drag; smaller capture area, no centerbody

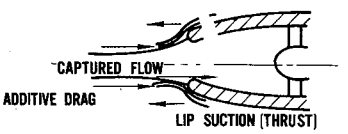

b) Supersonic inlet: at subsonic operation sharp lip eliminates benefit of lip suction; larger capture area because of centerbody

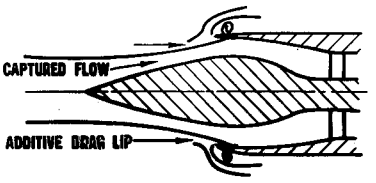

Fig. 2 Comparison of subsonic and supersonic inlets.

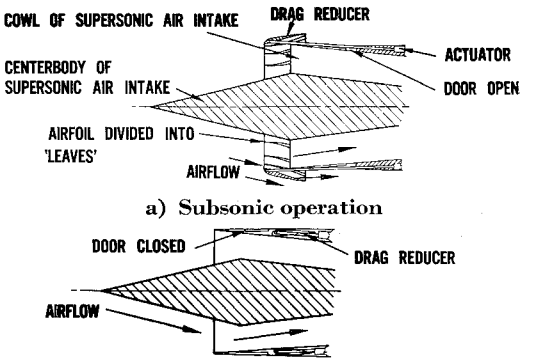

Fig. 3 Operation of drag-reducing airfoil.

the inlet drag also decreases. Of course, things are not quite so simple, since the lift-drag ratio of the airfoil depends on local Mach number and angle of attack. In general, however, the decrease in thrust does occur.

In choosing an airfoil for this application, the lift-drag ratio and lift coefficient were considered. It was expected that the Mach number range near the cowl lip was 0.8 to 1.0 at the Mach 0.85 freestream condition. Figure 5 shows the maximum lift-drag ratios and lift coefficients as a function of Mach number for NACA 64A004 and 10-10 airfoils.[1] It may be seen that the 10-10 airfoil has a much higher lift coefficient and its lift-drag ratio is superior in the Mach 0.9–1.0 range. The 10-10 airfoil was chosen because its high lift coefficient meant that it would be relatively small in size and because it was felt that the local Mach number would be too high for the 64A004 airfoil.

The airfoil was sized for an inlet having a 14° half-angle cone and a throat-capture area ratio of 0.65, and operating at a freestream Mach number of 0.85. It was assumed that the local flow angle would be about 12.5° and that the local dynamic pressure was equal to the freestream dynamic pressure. The local Mach number was assumed to be 0.95. The airfoil was set at 10° to the axis to obtain the optimum 2.5° angle of attack. The axial thrust coefficient desired was about 0.1, which should offset the additive drag of the inlet at choked flow. Thus, the plan form area was established.

Hinged-Cowl Theory of Operation

Another possibility for reducing the drag of supersonic inlets is to make the cowl in sections or "leaves" and hinge it so that it can be collapsed toward the center. By this means, some forebody suction can be created on the cowl leaves, and, in addition, the capture area is reduced, thus lowering the additive drag. The angle of the cowl in its collapsed position

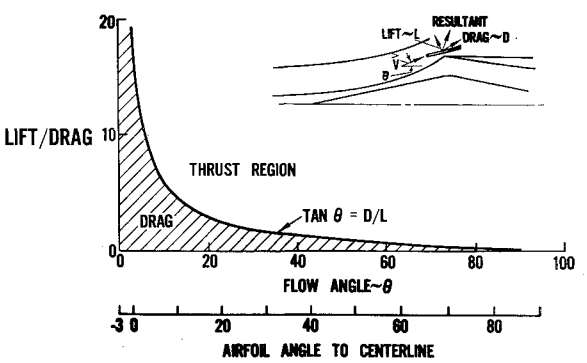

Fig. 4 Lift-drag ratio vs flow angle for any Mach number and any wing angle of attack. Assume: angle of attack $\alpha = 3$ is optimum.

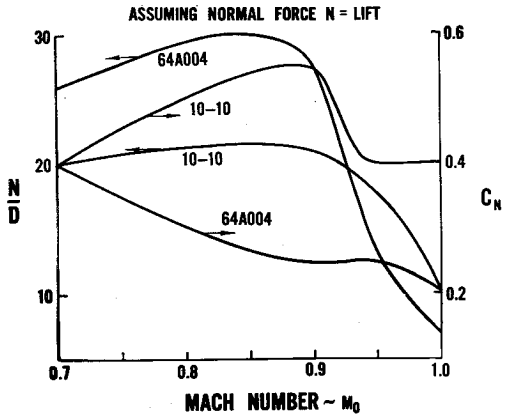

Fig. 5 Maximum lift-drag ratio and corresponding lift coefficient for transonic airfoils.

should be kept low so that the stagnation point is on the inside. Thus, high pressure recovery and low pressure drag will be attained.

Test Techniques

Wind Tunnel

The inlet drag studies were conducted in the 17- × 17-in. transonic wind tunnel located at the United Aircraft Research Laboratories. The tunnel is of the blowdown type with running times ranging from 0.5 to 1.5 min.

The tunnel test section has porous walls that eliminate wall interference effects on the model. A Mach number range of 0.35 to 1.4 is available by adjusting the pressure in a plenum around the test section.

Figure 6 shows the test section of the wind tunnel. The inlet models are supported from the hydraulically actuated sector, which permits variation of the model angle of attack. A 12-in.-diam multiple-source schlieren system is used to obtain schlieren photos of the test models through the perforated walls. Nominal test conditions were Mach 0.85 at 4100 psia total pressure. The total temperature was 540°R. Reynolds number based on a 4-in. inlet capture was 2.75×10^6.

Instrumentation

Digital data-recording systems using electric pressure transducers and strain-gage force balances record drag, flow, and pressure measurements. Data were processed on an IBM 7094, and printouts of various drag coefficients, total pressure

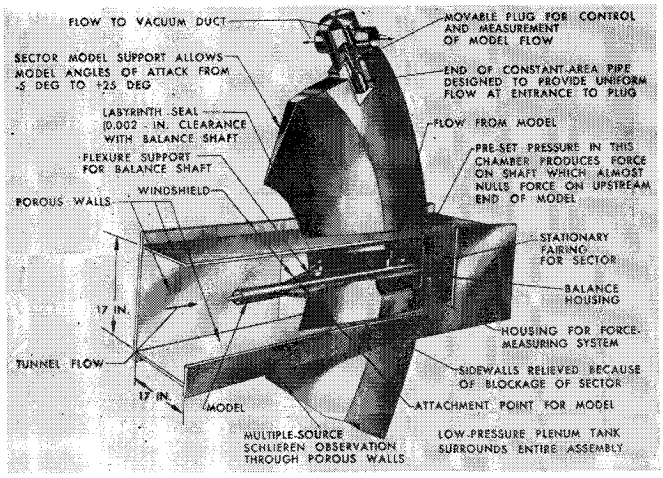

Fig. 6 Inlet model, balance, and support in 17-in. transonic tunnel.

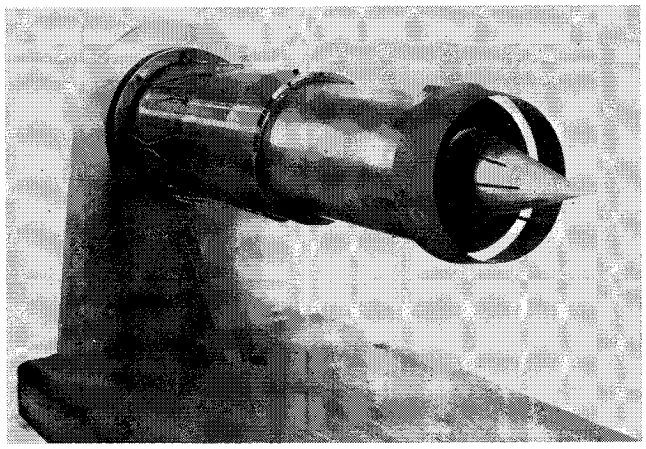

Fig. 7 Airfoil inlet model. (Throat-capture area ratio, 0.65; conical centerbody half-angle, 14°; drag-reducer airfoil angle from horizontal, 10°.)

recovery, relative weight flow, pressure ratios, etc., were available within hours.

The freestream Mach number was determined by measurement of the total pressure in the chamber preceding the tunnel nozzle, and the static pressure at a point 6 capture diam upstream of the inlet face. This point had been previously established as being undisturbed by changes in inlet flow. Inlet captured flow was varied and measured with a calibrated, movable-plug throttle. The throttle was choked at all times by maintaining a low back pressure. Thus, a pressure measurement upstream of the throttle and measurement of the throttle area were sufficient to obtain flow rates. With this throttle, a complete range of inlet flow was obtained during one blowdown run. Axial forces on the models were measured with a strain-gage force balance. The base of the balance was pressurized to approximately null the over-all force. A complete description of the equipment and procedures available in the transonic wind tunnel is available.[2]

Test Models

Airfoil Models

A series of transonic airfoils were tested on two axisymmetric inlet models. The airfoils were the NACA 10-10, 2% thick series. They were flat plates with elliptical leading and trailing edges. Major to minor axis ratio of the ellipses was 10. Three airfoils making 10°, 20°, and 30° angles with the inlet axis were used. These airfoils could be located in three axial positions as well, making a total of nine configurations. The two inlet models consisted of a sharp cylindrical cowl with a 14° and an 18° half-angle centerbody. The throat-capture area ratio was 0.65 for both inlets. Figure 7 is a photo of one of the models. A composite drawing of the airfoil models is shown in Fig. 8. The models were also tested at Mach 0.85 over the entire captured-flow range.

Hinged-Cowl Models

A series of axisymmetric inlet models were tested. One hinged cowl having a 10° droop angle and a capture-maximum area ratio of 0.77 was simulated on all models. Three conical centerbodies were used having a cone half-angle of 14° and three throat-capture area ratios (0.27, 0.42, and 0.57). Figure 9 shows the inlet model with the 0.42-area-ratio centerbody.

To measure cowl pressure drag, four pressure taps were located on the outside of the drooped portion of the cowl. One tap was located on the outside of the cylindrical portion. The inlets were tested at Mach 0.85 over the entire captured-flow range.

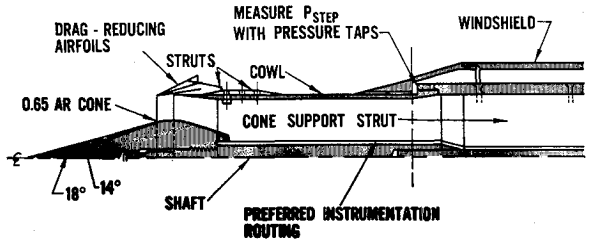

Fig. 8 Composite drawing of airfoil-inlet models.

Results of Airfoil Tests

The results of the airfoil drag tests are shown in Fig. 10. The sum of the additive drag and pressure drag coefficients are shown as a function of relative weight flow. Friction drag on the cowl was subtracted out. The results from all configurations are compared with the drag of the plain inlet. It was found that the drag of the struts that support the airfoil was negligible. The strut drag was determined by testing the inlet with the struts in place but without the airfoil. Thus, the change in drag is due entirely to the airfoils.

It can be seen that the 10° airfoil in the furthest forward position reduced the inlet drag the most. As the 10° airfoil was moved toward the cowl, the reduction of drag was diminished. It is also obvious that drag of the 20° and 30° airfoils was much higher than the 10° airfoil. With the 20° and 30° airfoils, the trend was opposite at high weight flows as they were moved toward the cowl. The drag was reduced. At low weight flow ratios, however, the trend is again similar to the 10° airfoil trend.

These results were caused by changes in the angle of attack relative to the local flow and by interference between the cowl and the airfoil. The interference between the cowl and the airfoil is caused by the formation of a divergent passage between them. At high weight flows, the entrance to the passage acts as a nozzle throat, and a supersonic region followed by a normal shock occurs in the passage. The resulting low pressure creates drag on the airfoil. This interference is obviously reduced by moving the cowl forward, since this decreases the airfoil area subjected to this low pressure.

The angle of attack relative to the local flow is reduced by moving the cowl forward, which reduces the thrust. Reducing the relative weight flow increases the angle of attack and the airfoil thrust. The combination of these effects apparently increases the thrust of the 10° airfoil as it is moved forward.

The maximum flow rate was suppressed by the airfoils. It was found that the suppression increased as the airfoils were moved forward. The 10° airfoils caused the most flow suppression of the three. The reason for this is shown in Fig. 11. The total pressure profile at the throat is shown at choked flow with and without the airfoil. It appears that, for this flow rate, the stagnation point occurs on the outside of the airfoil. Thus, overexpansion shocks and flow separation occurs on the inside of the airfoil, causing the total pressure losses.

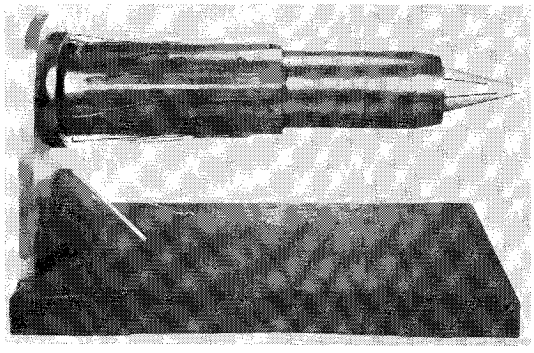

Fig. 9 Droop-cowl inlet model. (Throat-capture area ratio, 0.42; capture-maximum area ratio, 0.766; cowl droop angle from horizontal, 10°; centerbody half-angle, 14°.)

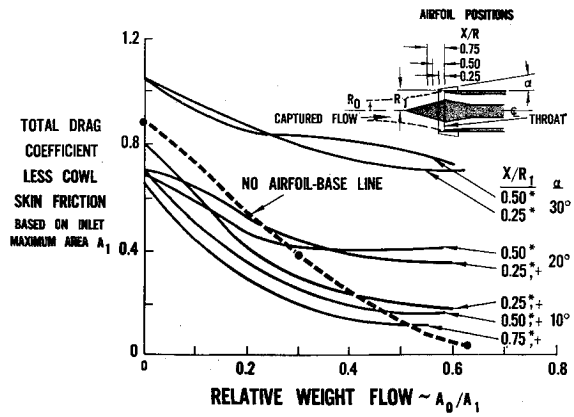

Fig. 10 Effect of airfoils on drag. (M_0, 0.85; cone half-angle, 14° (*), 18° (+); throat-capture area ratio, 0.65.)

Since both the additive drag and the pressure recovery of the airfoil-inlet combination are reduced, the maximum propulsion force F_p will probably not occur at the minimum drag point. As Fig. 11 shows, a radial flow distortion is introduced at the cowl lip, which will increase flow distortion at the engine face. Since the flow distortion is primarily radial, it probably is of secondary importance. The lower pressure recovery is the primary factor. An optimization of the airfoil operation cannot be attempted here without knowledge of the engine to be used and its pressure recovery and distortion influence coefficients.

It may be seen from Fig. 10 that none of the airfoils reduce the drag below the critical flow value for the plain inlet. It was also found that changing the cone half-angle from 14° to 18° had no effect on drag. The drag curves for both cone angles were identical for all airfoils tested. Thus, it appears that this change does not affect the flow around the cowl lip (at least at these area ratios).

Results of Drooped-Cowl Tests

The results of the drag tests on the drooped cowl are shown in Fig. 12. The sum of the coefficients of additive drag and cowl pressure drag are shown for three inlets with varying throat-capture area ratios and a 10° drooped cowl. The friction drag was subtracted out. Also shown for comparison are the drags for the same three inlets with the cowl swung out horizontally. It may be seen that the drag is much lower at the same weight flow when the cowl is swung in. Also, the drooped cowls reduce the maximum weight flow proportionally to the reduction in capture area from the undrooped position. It may be seen here, as in the airfoil test

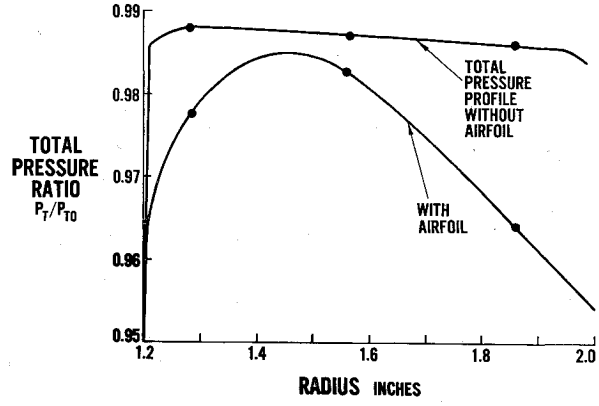

Fig. 11 Effect of airfoil on throat total pressure. ($\alpha = 10°$; $X/R = 0.25$; $W_R = W_{R_{CR}}$.)

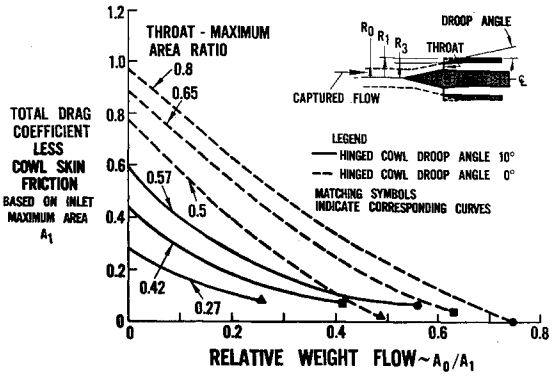

Fig. 12 Effect of hinged cowl on drag. (M_0, 0.85; cone half-angle, 14°; capture-maximum area ratio, 0.77; droop angle, 10°.)

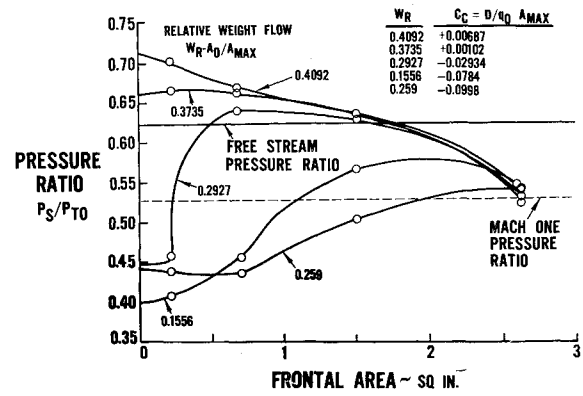

Fig. 14 Droop-cowl external pressure. (Cone angle, 14°; A_2/A_{max}, 0.42.)

results, that none of the droop-cowl drags are lower than the critical flow value for the undrooped-cowl inlet.

The reason for the reduction in drag obtained by the drooped-cowl inlets is the suction obtained on the cowl surface and the reduced additive drag due to the smaller capture area. Figures 13–15 show the pressure distributions and thrust coefficients obtained for the cowls at various weight flow ratios.

Although the flow is separated from the cowl, suction can still be attained. At the critical weight flow, however, stagnation occurs outside the cowl lip, creating high pressure and drag.

If the inlet centerbody is translatable, more mass flow could be captured by pulling the centerbody in. The critical mass flow could then be determined by some minimum area inside the cowl. The data shown in Fig. 12 could then be regarded as the drag for various axial positions of the centerbody, since the internal contours do not significantly affect the drag level. The drag curve is, of course, cut off at the same or a lower value of relative weight flow determined by internal choking.

If the cowl drag is subtracted from the total drag (minus friction), the additive drag for these drooped-cowl inlets can be obtained. These additive drags are shown in Fig. 16. Also shown are the additive drags obtained from straight cowl inlets.[3] It may be seen that, at throat-capture area ratios of 0.7 or higher, the two nearly coincide, whereas for lower area ratios, the drooped-cowl inlet has low additive drag at low flows and higher drag near the critical flow point. These results are supported by the fact that the cowl pressure waves should influence the upstream flow in a small region near the cowl lip. Then, as the cowl lip is moved away from the centerbody (increasing area ratio), the throat flow is less influenced by changes in cowl shape. Further, the changes in cowl shape are somewhat masked by a separation "bubble" on the outside caused by the sharp leading edge.

Concluding Remarks

It was demonstrated that the airfoil and the hinged-cowl modifications to supersonic inlets lower their drag in subsonic flight. However, at present, this occurs only for captured-flow rates below the maximum and involves a reduction in the maximum flow rate that the inlet can capture. Therefore, the drag reducers would work only when the design of the inlet and engine airflow requirements dictate that less flow than maximum must be captured at the subsonic flight condition.

The data do not preclude the possibility that drag could be reduced below the maximum flow rate value. The trends in the data indicate that airfoils with lower angles of attack and/or positioned further from the cowl may achieve this goal. Data on total pressure distribution at the throat for critical flow showed losses and total pressure distortion with the 10° airfoil. This indicates that the airfoil was operated at negative local attack angle and that the airfoil angle should be reduced.

With the drooped cowl, further drag reductions may be possible with changes in droop angle and/or capture-maximum area ratio. Since high pressures were obtained on the outside of the cowl at critical flow, it appears that a reduction in cowl droop angle will reduce the drag.

The airfoils and hinged cowl may have a supersonic drag penalty. This occurs because some volume in the cowl is required to store the airfoil and its actuator in supersonic flight. Similarly, storage volume is required for actuators for the hinged cowl. However, some or all of this storage space may already be available as dictated by other inlet design requirements.

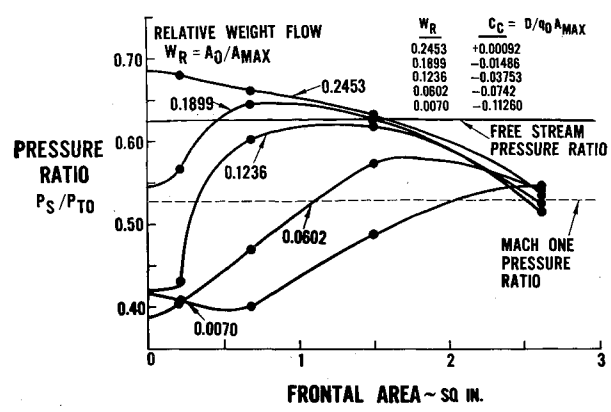

Fig. 13 Droop-cowl external pressure. (Cone angle, 14°; A_2/A_{max}, 0.27.)

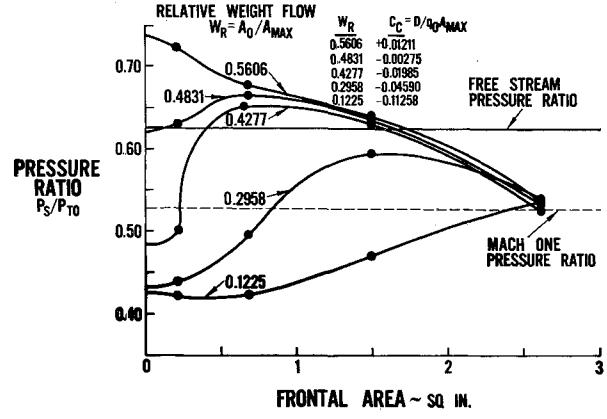

Fig. 15 Droop-cowl external pressure. (Cone angle, 14°; A_2/A_{max}, 0.57.)

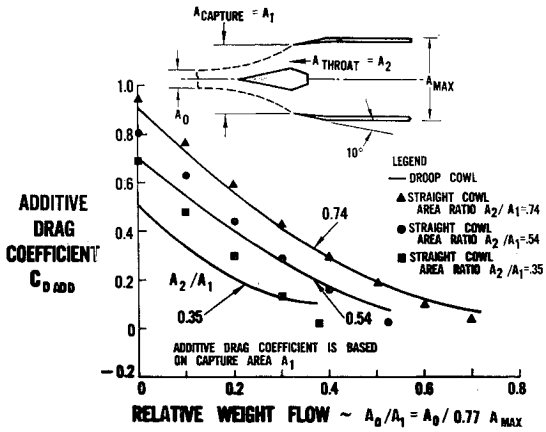

Fig. 16 Comparison between straight cowl and droop-cowl additive drag.

Although the inlets were not designed with good over-all pressure recovery in mind, some data were taken on cowl-lip pressure recovery for the airfoil tests. They indicate that, although additive drag is reduced, the maximum available net thrust F_A is also reduced because of pressure-recovery losses Thus, the maximum propulsive thrust F_p must be considered when optimizing an installation using the airfoil. Similar considerations apply to an installation using the drooped cowl.

The data also indicate that, for A_2/A_1 greater than 0.7, the cowl exterior shape tested did not change the additive drag. This means that cowl drag can be considered independently for cowl angles less than 10° and A_1/A_{max} less than 0.77, at least.

References

[1] Lindsey, W. F. and Landrum, E. J., "Flow and force characteristics of 2-percent-thick airfoils at transonic speeds," NACA RM L54I30 (January 1955).

[2] McLafferty, G. and Vergara, R., "Description of equipment and techniques used for inlet tests in UAC Research Dept. 17-inch blowdown tunnels," United Aircraft Research Labs. Rept. R-2000-30 (July 1957).

[3] Muller, G. L. and Gasko, W. F., "Subsonic-transonic drag of supersonic inlets," J. Aircraft **4**, 231–236 (1967).

[4] Petersen, M. W. and Tamplin, G. C., "Experimental review of transonic spillage drag of rectangular inlets," Air Force Aero Propulsion Lab., AFAPL-TR-66-30 (1966).

JULY-AUG. 1967 J. AIRCRAFT VOL. 4, NO. 4

A Segmented Wing Test Technique for Obtaining Spanwise Load Distributions

H. R. WASSON* AND T. E. MEHUS*
Northrop Corporation, Norair Division, Hawthorne, Calif.

A wind-tunnel test technique to determine the span loading on the wing of a complete aircraft configuration has been evolved and the data from a preliminary test series have been reduced to develop and to evaluate the method. The method is sufficiently inexpensive to be utilized during the early design phase of an airplane development. An existing model was modified by slitting the wing chordwise at seven spanwise stations leaving the spar intact and attaching strain gages to measure the wing bending moments. The reduction method used avoids the need to differentiate the bending-moment variation by curve-fitting the unknown span loading variation. A curve-fit polynomial with unknown coefficients is integrated, and a relationship is obtained between the bending moment and the unknown coefficients by a least-squares procedure. Data reduced by this technique are presented for typical test conditions. The accuracy of the method and means of improving the technique are discussed.

Nomenclature

a_{ij} = coefficients of $c_l c/\bar{c}$ in bending-moment equations
b = wing span
b_{ij} = coefficients of $c_l c/\bar{c}$ in least-squares equations
B_k = coefficients of kth power of curve-fit polynomial
c = local chord
$\bar{c}$ = mean chord
C_j = constant term of least-squares equations
c_l = local normal force coefficient
$c_l c/\bar{c}$ = span loading parameter
$\bar{C}_m(x_i)$ = estimated bending-moment coefficient at wing station i, bending moment/$\frac{1}{2}qSb$
$C_m(x_i)$ = test data bending moment coefficient at wing station i, bending moment/$\frac{1}{2}qSb$
l_i = ith Lagrangian interpolating polynomial
n = highest power in polynomial curve fit
q = dynamic pressure
S = wing area
W_i = weighting function at ith spanwise station
x = spanwise location from centerline
x_i = ith spanwise station
y = dependent variable in curve-fit polynomial $c_l c/\bar{c}$ or c_l
α = angle of attack, positive nose up
β = angle of sideslip, positive nose left
δ_a = angle of aileron deflection, positive trailing edge down

Subscripts

i, j, k = stations at which lift or moment is given or to be evaluated

Presented as Paper 66–768 at the AIAA Aerodynamic Testing Conference, Los Angeles, Calif., September 21–23, 1966; submitted October 3, 1966; revision received April 5, 1967. [6.01]

* Research Engineer, Vehicle Dynamics and Control Group.

Introduction

IN the design and analysis of airplanes, it is necessary that the distribution of the loading on the wing be known in order to perform the stress analysis. In addition, the span